

## Accepted Manuscript

Discovery of a potent orally bioavailable retinoic acid receptor-related orphan receptor-gamma-t (ROR $\gamma$ t) inhibitor, S18-000003

Yoshikazu Sasaki, Masahide Odan, Shiho Yamamoto, Shiro Kida, Masaya Shimizu, Takayo Haruna, Azumi Ueyama, Ayahisa Watanabe, Takayuki Okuno

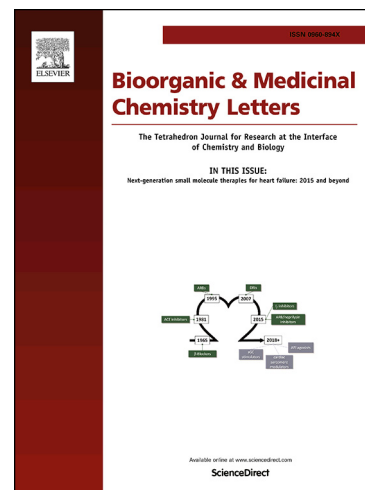
PII: S0960-894X(18)30774-1  
DOI: <https://doi.org/10.1016/j.bmcl.2018.09.032>  
Reference: BMCL 26053

To appear in: *Bioorganic & Medicinal Chemistry Letters*

Received Date: 12 August 2018  
Revised Date: 21 September 2018  
Accepted Date: 25 September 2018

Please cite this article as: Sasaki, Y., Odan, M., Yamamoto, S., Kida, S., Shimizu, M., Haruna, T., Ueyama, A., Watanabe, A., Okuno, T., Discovery of a potent orally bioavailable retinoic acid receptor-related orphan receptor-gamma-t (ROR $\gamma$ t) inhibitor, S18-000003, *Bioorganic & Medicinal Chemistry Letters* (2018), doi: <https://doi.org/10.1016/j.bmcl.2018.09.032>

This is a PDF file of an unedited manuscript that has been accepted for publication. As a service to our customers we are providing this early version of the manuscript. The manuscript will undergo copyediting, typesetting, and review of the resulting proof before it is published in its final form. Please note that during the production process errors may be discovered which could affect the content, and all legal disclaimers that apply to the journal pertain.



## Discovery of a potent orally bioavailable retinoic acid receptor-related orphan receptor-gamma-t (ROR $\gamma$ t) inhibitor, S18-000003

Yoshikazu Sasaki<sup>a\*</sup>, Masahide Odan<sup>a</sup>, Shiho Yamamoto<sup>a</sup>, Shiro Kida<sup>a</sup>, Masaya Shimizu<sup>a</sup>, Takayo Haruna<sup>a</sup>, Azumi Ueyama<sup>a</sup>, Ayahisa Watanabe<sup>a</sup> and Takayuki Okuno<sup>a</sup>

<sup>a</sup>Pharmaceutical Research Division, Shionogi & Co., Ltd., 1-1, Futaba-cho 3-chome, Toyonaka, Osaka 561-0825, Japan

\*Corresponding author. Tel.: +81 6 6331 6727.

E-mail address: [yoshikazu.sasaki@shionogi.co.jp](mailto:yoshikazu.sasaki@shionogi.co.jp) (Y. Sasaki)

### Keywords:

ROR $\gamma$ t inhibitor

Cocrystal structure with ROR $\gamma$ t LBD

Th17 cell

IL-17

Autoimmune disease

### Abstract:

The retinoic acid receptor-related orphan receptor-gamma-t (ROR $\gamma$ t) is the master transcription factor responsible for regulating the development and function of T-helper 17 (Th17) cells, which are related to the pathology of several autoimmune disorders. Therefore, ROR $\gamma$ t is an attractive drug target for such Th17-mediated autoimmune diseases. A structure–activity relationship (SAR) study of lead compound **1** yielded a novel series of ROR $\gamma$ t inhibitors, represented by compound **6**. Detailed SAR optimization, informed by X-ray cocrystal structure analysis, led to the discovery of a potent orally bioavailable ROR $\gamma$ t inhibitor **25**, which inhibited IL-17 production in the skin of IL-23-treated mice by oral administration.

T-helper 17 (Th17) cells, which were discovered as a unique T-helper cell lineage distinct from Th1 and Th2 cells,<sup>1</sup> produce the interleukin 17 (IL-17) family of cytokines in response to stimulation by interleukin 23 (IL-23). IL-23 is commonly associated with various human inflammatory and autoimmune disorders,<sup>2a</sup> including rheumatoid arthritis,<sup>2b</sup> inflammatory bowel disease,<sup>2c</sup> multiple sclerosis<sup>2d</sup> and psoriasis.<sup>2e</sup> The retinoic acid receptor-related orphan receptor-gamma-t (ROR $\gamma$ t) is a nuclear receptor that has been identified as a key regulator of Th17 cell differentiation. Therefore, ROR $\gamma$ t may be a potential drug target for IL-23/Th17-related autoimmune diseases.

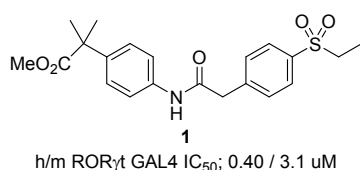
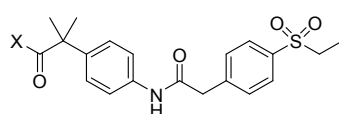


**Figure 1.** Structure of the SAR lead compound **1**.

Several ROR $\gamma$ t inhibitors have been reported by groups in industry and academia. There are also several reviews summarizing recent reports of discoveries of small molecule ROR $\gamma$ t modulators, including agonists and inverse agonists.<sup>3</sup> Among them, a series of ROR $\gamma$ t inhibitors have a 4-ethylsulfonylbenzyl moiety, which GSK originally disclosed and is now being pursued by several other companies.<sup>4,5,6,7</sup> Our group has also explored ROR $\gamma$ t inhibitors based on a high-throughput screening campaign. Subsequent hit-to-lead optimization of several chemotypes led to the identification of methyl ester derivative **1**, which also possesses the ethylsulfonylbenzyl structure (Figure 1). In this report, we describe the identification of a novel series of  $\alpha,\alpha$ -dimethylphenylacetamide ROR $\gamma$ t inhibitors, which were obtained by lead optimization of **1** through a structure–activity relationship (SAR) study and guided by a cocrystal structure analysis. These studies led to the discovery of a potent and orally bioavailable ROR $\gamma$ t inhibitor, S18-000003.

**Table 1.** SAR of amide derivatives of **1**.



Compd.	X	h/m ROR $\gamma$ t GAL4 IC <sub>50</sub> <sup>a</sup> ( $\mu$ M) [%eff] <sup>b</sup>	h ROR $\gamma$ t Binding IC <sub>50</sub> <sup>c</sup> ( $\mu$ M)
<b>1</b>	MeO	0.40 [93] / 3.1 [77]	0.064
<b>2</b>	Me	0.37 [89] / >10 [51]	0.030
<b>3</b>		0.18 [90] / >10 [52]	< 0.030
<b>4</b>		0.47 [89] / 10 [55]	0.033
<b>5</b>		0.43 [91] / >10 [50]	0.036
<b>6</b>		0.014 [93] / 0.47 [69]	< 0.030
<b>7</b>		0.014 [93] / 0.33 [76]	< 0.030
<b>8</b>		0.010 [93] / 0.11 [87]	< 0.030
<b>9</b>		0.26 [92] / 1.9 [84]	< 0.030

<sup>a</sup> Cell-based ROR $\gamma$ t-GAL4 promoter reporter assays.

<sup>b</sup> Percent efficacy denotes maximum inhibition activity.

<sup>c</sup> Competitive binding assays towards human ROR $\gamma$ t.

Our initial work on the lead compound **1** focused on converting the ester moiety of **1** to various amides (Table 1). The inhibition was measured in cell-based ROR $\gamma$ t-GAL4 promoter reporter assays, using human or mouse genes, and also by competitive binding assays towards human ROR $\gamma$ t (see SI for details). On the one hand, converting the methyl ester to alkyl amides **2**, **3**, **4** or **5** showed no significant activity improvement. On the other hand, anilide **6** was more than 6 times more potent than the methyl ester **1** in the mouse gene assay. *N*-methyl anilide **7** was as potent as **6**, suggesting that the NH-proton is not important for activity. Furthermore, indoline amide **8** is also acceptable and a more potent inhibitor than anilide **6**. However, isoindoline amide **9** decreased the inhibition activity. The binding assays demonstrated that all compounds of this chemotype inhibit ROR $\gamma$ t activity by binding to ROR $\gamma$ t ligand-binding domain (LBD).

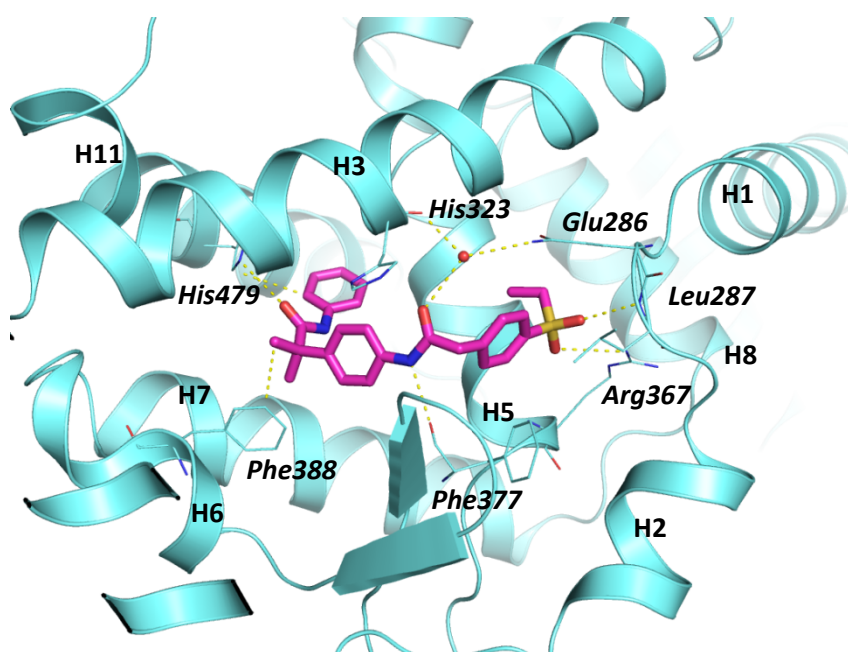


**Figure 2.** Cocystal structure of **6** in complex with human ROR $\gamma$ t LBD [PDB: 5ZA1].

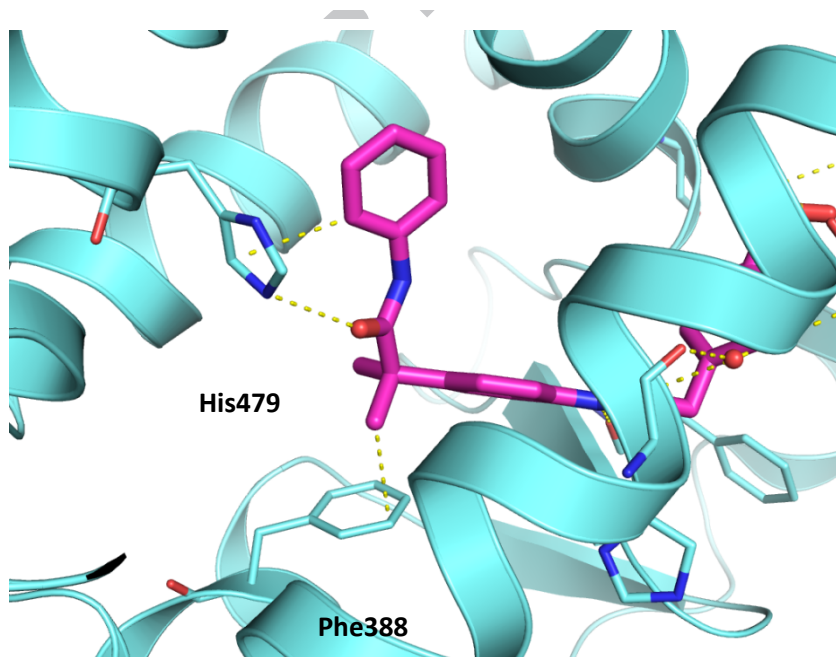


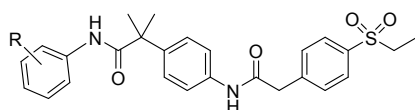
**Figure 3.** Binding mode around the dimethylmethylene linker of **6** [PDB: 5ZA1].

Our efforts to cocrystallize anilide **6** and the human ROR $\gamma$ t LBD revealed the binding mode at a resolution of 2.52Å (Figure 2, PDB: 5ZA1). The 4-ethylsulfonylbenzyl group of the ligand interacted with the protein residues via several hydrogen bonds. The ligand sulfone moiety formed two hydrogen bonds with the side chain of Arg367 and the backbone NH of Leu287. There are two water-mediated hydrogen bonds between the carbonyl moiety of **6**, the side chain of Glu286, and the backbone carbonyl of His323. Furthermore, the anilide N-H in the central part of the compound also formed a hydrogen bond with the backbone of Phe377. One of the methyl groups of the dimethyl methylene linker of the ligand interacted with the side chain of Phe388 via CH- $\pi$  interaction (Figure 3). The side chain of His479 formed a hydrogen bond with the carbonyl moiety of **6** and also engaged in an edge-to-face  $\pi$ - $\pi$  stacking interaction with the phenyl moiety of the compound. There was no interaction between the anilide proton and any residues in the protein, which explains the lack of inhibitory activity difference between N-H anilide compound **6** and *N*-methyl anilide **7**. His479 in helix 11 is thought to play a critical role in stabilizing the interaction of the activation function helix 2 (AF2 helix or helix 12) with coactivators by forming a hydrogen bond with Tyr502 and an edge-to-face  $\pi$ - $\pi$  interaction with Phe506 on AF2 helix.<sup>8</sup> The disruption of the His479-related interactions could cause the disorder of secondary structure for helix 11'-12 in the ROR $\gamma$ t LBD co-structure.<sup>9</sup>

The binding mode of the 4-ethylsulfonylbenzyl moiety of the ligand in the ROR $\gamma$ t LBD is similar to previously reported ROR $\gamma$ t ligands that also possess this moiety.<sup>5</sup> However, the dimethylmethylene linker made the anilide side of the molecule form a twisted structure in the ROR $\gamma$ t LBD, which caused the terminal anilide moiety to occupy a distinctive space in the binding pocket. In this pocket, a strong interaction between His479 and the ligand can be formed thereby causing the orientation of His479 to differ from that observed in a previously reported ROR $\gamma$ t agonist ligand cocrystal structure (PDB: 3L0L),<sup>8</sup> the previously reported cocrystal structures retain the three-dimensional structure of H11, H11' and H12 [PDB: 4XT9, 4NIE].<sup>5</sup> The interactions between the anilide moiety and His479 may be one of the critical interactions for the inhibition activity of this chemotype.

Next, we explored the SAR of the substitution pattern on the phenyl ring of the ligand again using cell-based reporter assays (Table 2). Adding a F group at the *o*- or *m*-position increased the inhibition activity (**10** and **11**).

**Table 2.** SAR of substituents on the terminal anilide ring.



Compd.	R	h/m ROR $\gamma$ t GAL4 IC <sub>50</sub> <sup>a</sup> (μM) [%eff] <sup>b</sup>	h/m Th17 IC <sub>50</sub> <sup>c</sup> (μM)	Metabolic stability Remaining (h, r %)
<b>6</b>	H	0.014 [93] / 0.47 [69]	ND / 0.48	8.5, 30
<b>10</b>	<i>o</i> -F	0.0044 [93] / 0.10 [76]	ND / 0.10	67, 19
<b>11</b>	<i>m</i> -F	0.0098 [94] / 0.26 [84]	ND / 0.29	2.7, 24
<b>12</b>	<i>p</i> -F	0.033 [93] / 0.55 [78]	ND / 1.1	75, 70
<b>13</b>	<i>o</i> -Me	0.14 [93] / 6.8 [57]	ND / ND	24, 6
<b>14</b>	<i>o,p</i> -Di-F	0.095 [91] / 1.8 [73]	0.036 / 1.3	97, 73

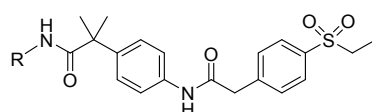
<sup>a</sup> Cell-based ROR $\gamma$ t-GAL4 promoter reporter assays.

<sup>b</sup> Percent efficacy denotes maximum inhibition activity.

<sup>c</sup> Inhibitory activity towards mouse and/or human Th17 differentiation.

Especially, *o*-F substitution caused a four-fold increase in potency compared with that of the non-substituted anilide **6** in the mouse reporter assay. However, the introduction of a Me group at the *o*-position caused more than a ten-fold loss of inhibition activity in the mouse ROR $\gamma$ t reporter assay (**13**). Inhibitory activity of each compound towards mouse and/or human Th17 differentiation was also assayed and found to be similar to that of the cell-based reporter assays. Furthermore, metabolic stability was also evaluated in both human and rat liver microsomes. Insertion of a F group into the *p*-position on phenyl moiety improved the metabolic stability, however it also decreased the inhibition activity (**12**, **14**).

**Table 3.** SAR of various terminal pyridyl amide derivatives.



Compd.	R	h/m ROR $\gamma$ t GAL4 IC <sub>50</sub> <sup>a</sup> (μM) [%eff] <sup>b</sup>	Solubility (pH1.2, 6.8, μM)	Metabolic stability Remaining (h, r %)
<b>6</b>	Phenyl	0.014 [93] / 0.47 [69]	46.9, 26.6	8.5, 30
<b>15</b>	2-pyridyl	0.040 [93] / 1.3 [73]	>50, >50	60, 36
<b>16</b>	3-pyridyl	0.15 [93] / 4.5 [63]	ND, ND	ND, ND
<b>17</b>	4-pyridyl	1.8 [87] / >10 [47]	>50, >50	4.3, 25

<sup>a</sup> Cell-based ROR $\gamma$ t-GAL4 promoter reporter assays.

<sup>b</sup> Percent efficacy denotes maximum inhibition activity.

For the purpose of improving the pharmacokinetic profile of **6**, we next performed a SAR with a terminal pyridine ring instead of a phenyl ring. We also evaluated the structure–solubility and structure–metabolic stability relationships (Table 3). It was revealed that 2-substituted pyridine moiety was superior in terms of inhibition activity, solubility and metabolic stability compared with that of **6** and all the other substitution patterns of pyridine.

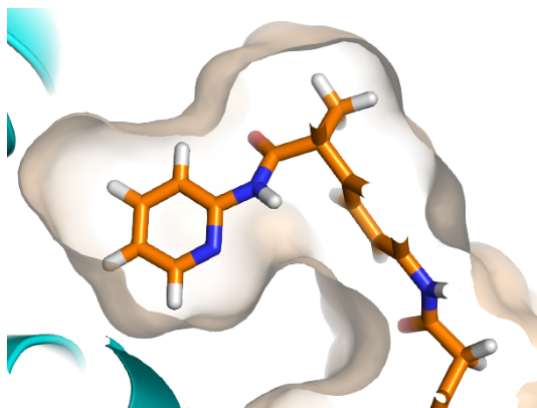
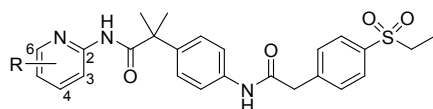


**Figure 4.** Predicted binding mode of **15**.

The SAR of the 2-substituted pyridine was explored with substitution on pyridine ring (Table 4). Prior to that, we predicted the binding mode of **15** using MD calculation with Maestro 11.1 (Figure 4). It was estimated that the pyridine and adjacent amide bond avoid the *syn* rotamer to prevent lone pair repulsion between amide carbonyl oxygen and pyridine nitrogen.<sup>10</sup> According to this predicted bind mode, there is space around the 4-position of the pyridine ring, which encouraged us to insert substituents into that position in this SAR study. Insertion of a F group

**Table 4.** SAR of substituents on the pyridine ring.



Compd.	R	h/m RORγt GAL4 IC <sub>50</sub> <sup>a</sup> (μM) [%eff] <sup>b</sup>	Solubility (pH1.2, 6.8, μM)	Metabolic stability Remaining (h, r %)
<b>15</b>	H	0.040 [93] / 1.3 [73]	>50, > 50	60, 36
<b>18</b>	4-F	0.031 [94] / 0.32 [86]	>50, > 50	69, 47
<b>19</b>	3-F	0.31 [92] / >10 [37]	>50, > 50	93, 80
<b>20</b>	4-CF <sub>3</sub>	0.025 [94] / 0.078 [94]	26, 0.50	36, 23
<b>21</b>	6-CF <sub>3</sub>	0.50 [90] / 5.4 [66]	1.1, 0.60	74, 71
<b>22</b>	4-Cl	0.0082 [95] / 0.10 [86]	>50, 4.7	40, 8.1
<b>23</b>	4-CN	0.040 [97] / 0.29 [91]	47, 25	92, 72

<sup>a</sup> Cell-based RORγt-GAL4 promoter reporter assays.

<sup>b</sup> Percent efficacy denotes maximum inhibition activity.

**(18)** increased the inhibition activity compared with that of **15**. Conversely, insertion of a F group at the 3-position (**19**) decreased the potency, probably because of the lack of space around the 3-position of the pyridine ring. Likewise, 4-CF<sub>3</sub> substituted pyridine compound **20** also had strong RORγt inhibitory activity, while 6-CF<sub>3</sub> substituted pyridine compound **21** decreased the inhibition activity compared with that of non-substituted pyridine **15**. Introduction of a Cl group to the 4-position gave analog **22**, which showed good inhibition activity, but it also showed unfavorable metabolic stability. The metabolic stability could be improved by 4-CN substitution and moderate RORγt inhibition activity was retained.<sup>11</sup>

Precise observation of the binding mode around the central aromatic ring of **6** suggested that there is some empty space over the 3-position of aniline ring, which prompted us to insert a substituent into that position (Table 5). Addition of a F group to the 3-position of **12** resulted in increased inhibition activity (**24**). Introduction of a F group into *o,p*-difluoro compound **14** and 4-cyanopyridine compound **23** also increased potency (**25**, **26**). Insertion of a F moiety into central phenyl ring maintained good metabolic stability of each compound. Other reports also note that introducing a Cl group to that position leads to increased potency.<sup>5a,6b</sup> Precise examination of substituents at this position has yet to be fully optimized in our research.

**Table 6.** Selectivity profile of inhibitors towards other ROR family members.

Compd.	h ROR $\alpha$ Binding IC <sub>50</sub> <sup>a</sup> ( $\mu$ M)	h ROR $\beta$ GAL4 IC <sub>50</sub> <sup>b</sup> ( $\mu$ M)	h LXR $\alpha/\beta$ GAL4 EC <sub>50</sub> <sup>c</sup> ( $\mu$ M)
<b>12</b>	>10	>10	>30 / >30 <sup>d</sup>
<b>24</b>	>10	>10	>30 / >30 <sup>d</sup>
<b>25</b>	>10	>10	>30 / >30 <sup>d</sup>
<b>26</b>	>10	>10	>30 / >30 <sup>d</sup>

<sup>a</sup> Competitive binding assays towards human ROR $\alpha$ .

<sup>b</sup> Cell-based human ROR $\beta$ -GAL4 promoter reporter assays.

<sup>c</sup> Cell-based human LXR $\alpha/\beta$ -GAL4 promoter reporter assays.

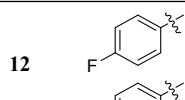
<sup>d</sup> No agonist activity on both LXR $\alpha$  and LXR $\beta$  was observed up to 30  $\mu$ M.

A selection of compounds were evaluated towards other members of the ROR family, as shown in Table 6, to demonstrate selectivity for ROR $\gamma$ t. None of these compounds bound to human ROR $\alpha$  LBD, repressed human ROR $\beta$  transcriptional activity or had human LXR $\alpha/\beta$  agonist activity.

**Table 7.** Pharmacokinetic properties of compounds in rats.

Compd.	iv, 0.5 mg/ kg				po, 1 mg/ kg				
	AUC <sub>iv</sub> (ng · h/mL)	CL <sub>tot</sub> (mL/min/kg)	t <sub>1/2</sub> (h)	Vd <sub>ss</sub> (L/kg)	C <sub>max</sub> (ng/mL)	AUC <sub>po</sub> (ng · h/mL)	T <sub>max</sub> (h)	BA (%)	fu (%)
<b>24</b>	986	8.45	2.5	1.7	85.3	786	2.5	39.9	3.6
<b>25</b>	1930	4.33	3.2	1.1	185	2110	4	54.5	3.4
<b>26</b>	556	15.0	2.9	3.3	33.3	218	1	19.6	5.1

Compd.	R1	R2	h ROR $\gamma$ t Binding IC <sub>50</sub> <sup>a</sup> ( $\mu$ M)	h/m ROR $\gamma$ t GAL4 IC <sub>50</sub> <sup>b</sup> ( $\mu$ M) [%eff] <sup>c</sup>	h/m Th17 IC <sub>50</sub> <sup>d</sup> ( $\mu$ M)	Solubility (pH1.2, 6.8, $\mu$ M)	Metabolic stability Remaining (h, r %)
--------	----	----	--	--	--	-------------------------------------	---



H

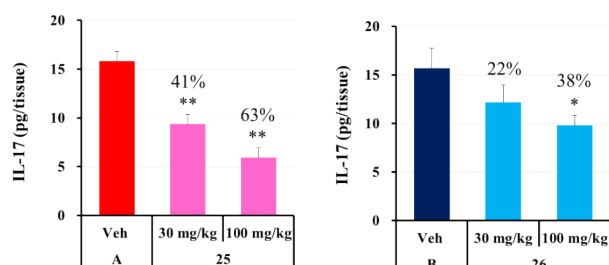
< 0.030

0.033 [93] / 0.55 [78]

0.024 / 1.1

39, 31

75, 70



Values represent the mean  $\pm$  SEM of 4-8 mice per group.

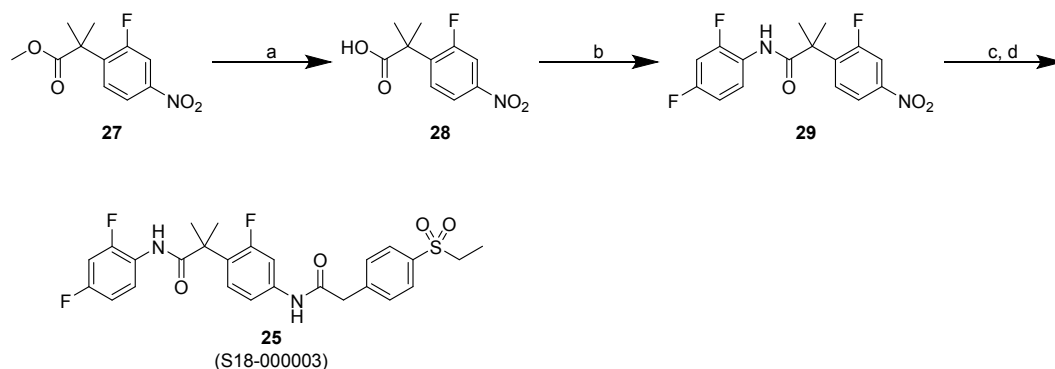
Percent efficacy denotes inhibition of IL-17 production relative to vehicle control.

\*\* p < 0.01 versus vehicle (Student's t-test)

**Figure 5.** Effect of **25** and **26** on IL-23-induced IL-17 production in mice.

Before *in vivo* pharmacological studies were performed, compounds **24**, **25** and **26**, which all have decent ROR $\gamma$ t inhibition activity as well as good solubility and metabolic stability, were profiled by rat-based pharmacokinetic studies (Table 7). Compound **26** having the largest distribution volume and the lowest *in vitro* metabolic stability among these compounds showed the highest total clearance, while **25** with the lowest distribution volume and the highest *in vitro* metabolic stability resulted in the lowest total clearance and the highest bioavailability.

On the basis of the *in vitro* efficacy against mouse Th17 differentiation and the *in vivo* PK profile, compounds **25** and **26** were selected for further biological evaluation. The effect of these compounds on IL-17 production in the skin of mice injected with IL-23 is shown in Figure 5. Oral administration of both compounds inhibited IL-17 production in the skin in a dose-dependent manner. Compound **25** showed significant inhibition at a dose of more than 30 mg/kg, and administration at a dose of 100 mg/kg resulted in 63% inhibition relative to vehicle controls. Conversely, IL-17 production in mice dosed with 100 mg/kg of **26** was inhibited by only 38% relative to vehicle controls, while **26** was 3-times more potent than **25** against mouse Th17 differentiation, *in vitro*. This is probably due to the difference between their pharmacokinetic profiles, *in vivo*.<sup>12</sup>



**Scheme 1.** Reagents and conditions: (a) LiOH, H<sub>2</sub>O, MeOH, 50 °C, (76%); (b) NBS, PPh<sub>3</sub>, DCM, 0 °C then 2,4-difluoroaniline, pyridine, r.t., (95%); (c) H<sub>2</sub>, Pd/C, EtOAc, r.t.; (d) 4-(ethylsulfonyl)benzeneacetic acid, HATU, Et<sub>3</sub>N, DMF, r.t., (2 steps 98%).

The synthesis of **25** (S18-000003) as a representative example is shown in scheme 1. Saponification of commercially available methyl ester **27** gave carboxylic acid **28**. Activation of carboxylic acid **28** with NBS and PPh<sub>3</sub> and simultaneous nucleophilic insertion of 2,4-difluoroaniline gave amide **29** in good yield.<sup>13</sup> The condensation conditions are conducive for insertion of less-nucleophilic aromatic amines. Reduction of nitro group on **29** followed by amide formation with HATU gave the desired compound, **25** in good yield.

In summary, we have identified a novel series of  $\alpha,\alpha$ -dimethylphenylacetamide ROR $\gamma$ t inhibitors which have a unique binding mode in cocrystal with ROR $\gamma$ t LBD protein. Oral administration of these compounds, represented by S18-00003, inhibited IL-17 production in the skin of IL-23-treated mice in a dose-dependent manner. Full details of the SAR studies of the series and proof-of-concept studies using a psoriasis disease model animal will be reported in due course.

## Acknowledgments

We thank Kei Takiyama for his great contribution to the basic SAR study in this research, and Yuki Tachibana and Mina Yamamoto for their helpful discussions. We are also grateful to Kazutaka Sekiguchi and Yuki Murakami for supporting the ADME experiments, and Atsuko Nishigaki, Akira Ueda, Nobuyuki Tai and Hiroki Naruse for their great contributions to the biological studies. We are also indebted to Azusa Nozu for her great help with MD calculation with Maestro. We thank James Murray, PhD from Edanz Group ([www.edanzediting.com/ac](http://www.edanzediting.com/ac)) for editing a draft of this manuscript.

## References and notes

- Langrish, C. L., Chen, Y., Blumenschein, W. M., Mattson, J., Basham, B., Sedgwick, J. D., McClanahan, T., Kastelein, R. A., Cua, D. J. *J. Exp. Med.* 2005;201:233-240.
- (a) Tang, C., Chen, S., Qian, H., Huang, W. *Immunology* 2012;135:112-24; (b) Lubberts, E. *Nat. Rev. Rheumatol.* 2015;11:415-29; (c) Cătană, C., Neagoe, I. B., Cozma, V., Magdaş, C., Tăbăran, F., Dumitraşcu, D. L. *World J. Gastroenterol.* 2015;21: 5823-30; (d) Jadidi-Niaragh, F., Mirshafiey, A. *Scand. J. Immunol.* 2011;74:1-13; (e) Cesare, A. D., Meglio, P. D., Nestle, F. O. *J. Invest. Dermatol.* 2009;129:1339-50.
- (a) Fauber, B. P., Magnuson, S. J. *Med. Chem.* 2014;57:5871-92; (b) Cyr, P., Bronner, S. M., Crawford, J. J. *Bioorg. Med. Chem. Lett.* 2016;26:4387-93; (c) Bronner, S. M., Zbieg, J. R., Crawford, J. J. *Expert Opin. Ther. Pat.* 2017;27:101-12; (d) Pandya, V. B., Kumar, S., Sachchidanand, S., Sharma, R., Desai, R. C. *J. Med. Chem.* 2018; Article ASAP, DOI: 10.1021/acs.jmedchem.8b00588.
- Zhang, W., Zhang, J., Fang, L., Zhou, L., Wang, S., Xiang, Z., Li, Y., Wisely, B., Zhang, G., An, G., Wang, Y., Leung, S., Zhong, Z. *Mol. Pharmacol.* 2012;82:583-90.

5. (a) Yang, T., Liu, Q., Cheng, Y., Cai, W., Yang, L., Wu, Q., Orband-Miller, L. A., Zhou, L., Xiang, Z., Huxdorf, M., Zhang, W., Zhang, J., Xiang, J.-N., Leung, S., Qiu, Y., Zhong, Z., Elliott, J. D., Lin, X., Wang, Y. *ACS Med. Chem. Lett.* 2014;5:65-68; (b) Wang, Y., Yang, T., Liu, Q., Ma, Y., Yang, L., Zhou, L., Xiang, Z., Cheng, Z., Lu, S., Orband-Miller, L. A., Zhang, W., Wu, Q., Zhang, K., Li, Y., Xiang, J.-N., Elliott, J. D., Leung S., Ren, F., Lin, X. *Bioorg. Med. Chem.* 2015;23:5293-302.
6. (a) Wang, Y., Cai, W., Zhang, G., Yang, T., Liu, Q., Cheng, Y., Zhou, L., Ma, Y., Cheng, Z., Lu, S., Zhao, Y.-G., Zhang, W., Xiang, Z., Wang, S., Yang, L., Wu, Q., Orband-Miller, L. A., Xu, Y., Zhang, J., Gao, R., Huxdorf, M., Xiang, J.-N., Zhong, Z., Elliott, J. D., Leung, S., Lin, X. *Bioorg. Med. Chem. Lett.* 2014;22:692-702; (b) Wang, Y., Cai, W., Cheng, Y., Yang, T., Liu, Q., Zhang, G., Meng, Q., Han, F., Huang, Y., Zhou, L., Xiang, Z., Zhao, Y.-G., Xu, Y., Cheng, Z., Lu, S., Wu, Q., Xiang, J.-N., Elliott, J. D., Leung, S., Ren, F., Lin, X. *ACS Med. Chem. Lett.* 2015;6:787-92; (c) Wang, Y., Cai, W., Tang, T., Liu, Q., Yang, T., Yang, L., Ma, Y., Zhang, G., Huang, Y., Song, X., Orband-Miller, L. A., Wu, Q., Zhou, L., Xiang, Z., Xiang, J.-N., Leung, S., Shao, L., Lin, X., Lobera, M., Ren, F. *ACS Med. Chem. Lett.* 2018;9:120-24; (d) Huang, Y., Yu, M., Sun, N., Tang, T., Yu, F., Song, X., Xie, Q., Fu, W., Shao, L., Wang, Y. *Eur. J. Med. Chem.* 2018;148:465.
7. (a) Gege, C. *Expert Opin. Ther. Pat.* 2016;26:737-44; (b) Chaudhari, S. S., Thomas, A., Khairatkar-Joshi, N., Bajpai, M. WO2013171729A2, 2013; (c) Sharma, R., Sahu, B., Mali, S. V., Singh, D., Kumar, P. B., Dawange, M., Mistry, H. WO2015145371A1, 2015; (d) Nagamochi, M., Gotanda, T., Goto, T., Sasaki, J., Yoshino, T., Isobe, T. JP2016128387A, 2016; (e) Zhong, X., Liu, B., Xue, Y., Li, X., Wang, F., He, W., Chen, X., Zhang, Y., Zheng, C. CN106187838A, 2016; (f) Morphy, J. R. WO2017044410A1, 2017; (g) Brunette, S. R., Csengery, J., Hughes, R. O., Li, X., Sibley, R., Turner, M. R., Xiong, Z. WO2017058831A1, 2017; (h) Lever, S., Narjes, F., Olsson, R. I., Von Berg, S. WO2017102784A1, 2017; (i) Desai, R., Kumar, S. S., Pandya, V., Desai, J., Raval, S. WO2018011747A1, 2018; (j) Yamamoto, S., Shirai, J., Kono, M., Shiokawa, Z., Yukawa, T., Imada, T., Negoro, N., Oda, T., Sasaki, S., Nara, Y.; Suzuki, S., Sato, A., Ishii, N., Shibuya, A., Nakagawa, Y., Cole, D., Gibson, T., Ivetac, A., Swann, S., Tyhonas, J. WO2018030550A1, 2018.
8. Jin, L., Martynowski, D., Zheng, S., Wada, T., Xie, W., Li, Y. *Mol Endocrinol.* 2010;24:923-29.
9. Fauber, B. P., Rene, O., de Leon Boenig, G., Burton, B., Deng, Y., Eidenschenk, C., Everett, C., Gobbi, A., Hymowitz, S. G., Johnson, A. R., La, H., Liimatta, M., Lockey, P., Norman, M., Ouyang, W., Wang, W., Wong, H. *Bioorg. Med. Chem. Lett.* 2014;24:3891-7.
10. Brameld, K. A., Kuhn, B., Reuter, D. C., Stahl, M. *J. Chem. Inf. Model.* 2008;48:1-24.
11. Jones, L. H.; Summerhill, N. W.; Swain, N. A.; Mills, J. E. *Med. Chem. Commun.* 2010;1:309-18.
12. The effect of ROR $\gamma$ t inhibitors on IL-23-induced IL-17 production in mice depended on IL exposure dose as well as inhibitory activity on Th17 differentiation. Discrete PK profiles of the compounds are shown in the supporting information.
13. Froyen, P. *Tetrahedron Lett.* 1997;38:5359-62.

## Supplementary Material

Supplementary data associated with this article can be found, in the online version, at <http://dx.doi.org/xxxxxxx>.

**Graphical Abstract**

To create your abstract, type over the instructions in the template box below.  
Fonts or abstract dimensions should not be changed or altered.



ACCEPTED MANUSCRIPT

- Highly potent ROR $\gamma$ t inhibitors discovered by a precise SAR study.
- Detailed binding mode discussion of the compound guided by X-ray cocrystal structure analysis.
- Compounds in the series inhibited IL-17 production in the skin of IL-23-treated mice by oral administration.

ACCEPTED MANUSCRIPT